Journal of Controlled Release 374 (2024) 254–266

Contents lists available at ScienceDirect

Journal of Controlled Release

journal homepage: www.elsevier.com/locate/jconrel

An *in situ* bioadhesive foam as a large intestinal delivery platform for antibody fragment to treat inflammatory bowel disease

Wunan Zhang [a], Fiona McCartney [b], Yining Xu [a], Cécilia Bohns Michalowski [a], Inês Domingues [a], Espoir K. Kambale [a], Tom G. Moreels [c], Léo Guilbaud [a], Cheng Chen [a], Valentina Marotti [a], David J. Brayden [b], Ana Beloqui [a,d,*]

[a] UCLouvain, Université catholique de Louvain, Louvain Drug Research Institute, Advanced Drug Delivery and Biomaterials, 1200 Brussels, Belgium
[b] University College Dublin School of Veterinary Medicine and Conway Institute, Belfield, Dublin D4, Ireland
[c] UCLouvain, Université Catholique de Louvain, Institute of Experimental and Clinical Research, Laboratory of Hepato-Gastroenterology, 1200 Brussels, Belgium
[d] WEL Research Institute, Avenue Pasteur, 6, 1300 Wavre, Belgium

ARTICLE INFO

Keywords:
Inflammatory bowel disease
Colonic drug delivery
Foam
Biologics
Gas intestinal permeation enhancer

ABSTRACT

Biologics have been widely used as injectables in the treatment of inflammatory bowel disease (IBD). Different local treatment attempts have been developed in recent years. However, maintaining systemic levels of biologics is still crucial for achieving colitis remission. An equilibrium between systemic and local concentrations of biologics is therefore essential for treatment of colitis. Current formulations struggle to create optimal balance between drug concentrations in plasma and the colonic wall. Addressing this challenge, we developed a rectally delivered *in situ* foam that generates CO_2 *via* a reaction between potassium bicarbonate (PB) and citric acid (CA) without the aid of an external device. An anti-TNF-α antibody fragment (Fab) was loaded into the foam formulation, which promoted prolonged colon retention and improved Fab distribution up to proximal colon following rectal administration to mice. In addition, we observed increased plasma Fab concentrations in mice receiving the rectal Fab foam compared to a Fab solution. In a non-everted rat gut *ex vivo* model, a single exposure to the CO_2-containing foam improved macromolecule transepithelial flux across colonic tissue by over ten-fold. Foam efficacy for Fab was investigated in a range of colitis mouse models, from acute to chronic. This non-invasive formulation platform demonstrates potential to overcome existing limitations in delivering biologics to inflamed colonic tissue.

1. Introduction

Inflammatory Bowel Disease (IBD) comprising of Crohn's disease, ulcerative colitis and indeterminate colitis is a chronic condition characterized by a pattern of relapsing and remitting episodes.[1] It presents a spectrum of symptoms including abdominal pain, diarrhea, rectal bleeding, and weight loss.[2] IBD necessitates lifelong medication and, in severe cases, surgical intervention, substantially impeding patient life quality. The global incidence of IBD is on the rise,[3–5] positioning it as a looming health challenge worldwide. Despite extensive research, the precise etiology of IBD remains unknown, and as of now, there is no cure. Biologics such as anti-TNF-α antibodies have been utilized as the next stage drugs to induce remission in moderate-to-severe disease.[6,7] They are considered the best options for IBD patients who fail to respond to small molecule drugs such as mesalamine, thiopurines or methotrexate.[6] However, current biological formulations require invasive administration routes and carry the potential risk of severe side effects, including infusion reactions, infections, and malignancies.[8] On the other hand, achieving systemic levels of biologics has been correlated with mucosal healing in IBD patients.[9,10] Development of a non-injected biologic formulation capable of achieving high local concentrations in the inflamed colon along with adequate systemic levels would be an advance in IBD management.

Foams are dispersions of gas within a liquid or solid phase,[8] which have extensive application in the pharmaceutical and cosmetic industries.[11] For IBD treatment, rectal foam formulations have been successfully used to deliver small molecule therapeutics including budesonide to treat ulcerative colitis of the sigmoid and transverse

* Corresponding author at: UCLouvain, Université catholique de Louvain, Louvain Drug Research Institute, Advanced Drug Delivery and Biomaterials, 1200 Brussels, Belgium.
E-mail address: ana.beloqui@uclouvain.be (A. Beloqui).

https://doi.org/10.1016/j.jconrel.2024.08.023
Received 16 May 2024; Received in revised form 22 July 2024; Accepted 13 August 2024

colon.[12] However, the integration of biologics into foam formulations for IBD treatment has been less explored. This gap is possibly due to the challenges posed by traditional foam production methods, where the turbulence from pumps and propellants can lead to the aggregation of biologic molecules, diminishing their bioactivities.[13] To surmount this challenge, we selected an alternative gas generation method and devised an *in situ* foam formulation employing a simple chemical reaction. It is a two part formulation mixture. Specifically, we devided a pre-foam solution into an acidic part containing citric acid (CA) and a basic part containing potassium bicarbonate (PB). The mixture of the two phases in the colon generates carbon dioxide (CO_2), thereby enabling formation of the foam.

We selected a murine anti-TNF-α antibody fragment (Fab, molecular weight (Mw) 47.8 kDa)) as a model biologic. We characterized the foam formulation, ensuring that the activity and the stability of the Fab was preserved during the foaming process. Through evaluation of the local retention, distribution and absorption from *in vivo* studies, we demonstrated that the foam increased the retention of the Fab at the colonic region, while enhancing systemic absorption. The therapeutic effects of the Fab-entrapped foam formulation were tested in several murine colitis models, differing in the degree of severity of the disease. *Ex vivo* studies were carried out in isolated rat colonic mucosae to investigate the potential permeation enhancement effect of the foam in the colonic delivery, comparing the effect to an established gold standard intestinal permeation enhancer (sodium caprate (C_{10})).

2. Methods

2.1. Materials

A murine anti-TNF-α fragment antibody (Fab) was obtained from UCB under a MTA agreement. Gelot™ 64, Tefose® 63 and Sedefos™ 75 were gifts from Gatefossé, France. Tween® 20, gelatin, sodium bicarbonate, sodium azide, sodium carbonate, potassium bicarbonate, gelatin, potassium bicarbonate, *O*-dianisidine, guanidine chloride and fluorescein isothiocyanate (FITC)-dextran (FD) were purchased from Sigma-Aldrich, USA. Silica nanoparticle (50 nm silica nanospheres, standard) was purchased from Nanocomposix, USA. Mouse TNF-α, ELISAPOT, streptavidin-horseradish peroxidase, Tris-HCl, sodium deoxycholic acid, sodium chloride, 3,3′,5,5′-Tetramethylbenzidine (TMB) substrate, EDTA, 2,4,6-Trinitrobenzene sulfonic acid (TNBS) and hexadecyltrimethylammonium bromide (HTAB) were purchased from Thermo Fisher Scientific, IL, USA. Dextran sodium sulphate (DSS) was purchased from Tdb Labs., Sweden. Triton X-100 was purchased from Carl Roth GmbH, Germany. SDS (Electrophoresis purity reagent) was purchased from Bio-Rad Laboratories, Japan. Protease inhibitor cocktail tablets were purchased from Roche Diagnostics GmbH, Germany.

2.2. Foam preparation

To prepare the *in situ* foam, PB was dissolved in phosphate buffer saline (PBS) to yield different concentrations (2 M (200 g/L) and 3 M (300 g/L)) as basic pre-foam solution. The acidic pre-foam solution was prepared by mixing the emulsifier (Gelot™ 64 and Tween® 20) and a different volume of 3 M citric acid. Gelot™ 64 was melted at 75 °C and mixed with Tween® 20 in a mass ratio of 1:5 emulsifier mixture. The citric acid solution was prepared by dissolving gelatin in CA (3 M) in MiliQ water at 75 °C with stirring at 200 rotations per min, followed by dilution with a silica nanoparticle solution (10 mg/mL in Mili-Q water) and Milli-Q water to achieve different citric acid concentrations (1 M and 2 M). The final citric acid solution contained gelatin (200 mg/mL) and silica nanoparticles (3 mg/mL). The emulsifier and the citric acid solution were then mixed at a mass to volume ratio of 1:4 at 75 °C with stirring at 100 rotations per min to produce the acidic pre-foam solution. The acidic and basic pre-foam solutions were mixed at a 1:1 volume ratio. The mixture of PB (3 M) basic part and CA (1.6 M) acidic part was referred to as foam (F), while the mixture of PB (2 M) basic part and CA (0.8 M) acidic part was referred as "low" foam (LF) (referring to lower concentrations of CO_2 content).

The anti-TNF-α Fab was incorporated into the formulation. The external buffer of the Ab fragment was first replaced with the basic solution of the foam. This was accomplished using a 10 kDa ultrafiltration membrane and subjecting the mixture to a speed of 5000 g for 10 min at 4 °C. This process was repeated for a total of 8 cycles. The Fab in foam or LF pre-foam solution were stored at 4 °C until further utilization.

2.3. Foam characterization

Foam expansion was measured using a scaled falcon tube. Specifically, acidic pre-foam solution (200 μL) and basic pre-foam solution (200 μL) were mixed at 37 °C. The volume of the resulting foam was measured over time, and the maximum expanded volume was recorded. The point at which the foam completely disappeared was used as an indicator of its stability.

Subsequently, the materials underwent microscopic characterization to investigate the bubble formation within the foam using a Zeiss microscopy (Discovery V12, Carl Zeiss, Germany). The size distribution of the bubbles was assessed by mixing the acidic foam phase (40 μL) with the basic foam phase (40 μL) on a glass slide. Serial microscopy was then performed for both of the foam and LF at designated times to evaluate the morphology of the bubbles over time.

To assess the feasibility of incorporating the Fab into the basic pre-foam solution, the stability of the Fab was investigated in different ways. Fab in pre-foam basic solution and pre-LF basic solution were stored at 4 °C (25 mg/mL).

Fab aggregation was evaluated by examining its UV spectrum. The UV spectrum of diluted Fab (2 mg/mL) was recorded using a NanoDrop™ 2000/2000c Spectrophotometer (Thermo Fisher Scientific Inc., USA). In addition, the UV absorbance at 340 nm was specified to investigate the turbidity of the antibody over time. The UV spectrum and turbidity of the Fab in basic pre-foam solutions were compared to that of the freshly thawed antibody in its original buffer.

The conformational stability of the Fab was studied *via* intrinsic fluorescence spectrum as previously described.[14] The Fab in basic foam solution and freshly thawed Fab were both diluted (200 μg/mL). To prepare the unfolded Fab, guanidine chloride (6 M) was used to dilute the Fab (200 μg/mL) and incubated at room temperature for 10 min. The fluorescence spectrums of the Fab were then measured by a SpectraMax® using an excitation wavelength of 280 nm and an emission wavelength ranging from 310 nm to 410 nm. The maximum emission wavelength of the antibody in the basic foam solution was compared to that of the freshly thawed Fab and the unfolded antibody.

The binding affinity of the Fab procured post-foaming process was evaluated by mixing the basic foam solution (20 μL) with the acidic foam phase (20 μL). The mixture was then incubated at 37 °C for 30 min. Then, 960 μL of PBS was added to dissolve the foam followed by vortexing. The foam dilution was centrifuged at 5000 *g* for 15 min and the supernatant was collected to measure the antibody activity using the following method with a self-modified competitive ELISA. TNF-α was dissolved in a coating buffer (50 μg/mL, composed of 1.59 mg/mL $NaHCO_3$, 2.94 mg/mL Na_2CO_3 and 0.5 mg/mL NaN_3). The TNF-α solution (100 μL) was added into 96-well plates and incubated at 4 °C overnight. The plate was then washed thrice with 0.05% (*v*/v) Tween® 20 and blocked with ELISAPOT for 2 h. Fab in foam (FabF) and Fab in low foam (FabLF) post-foaming solution were serially diluted (concentrations ranging from 200 μg/mL to 25 ng/mL), alongside freshly thawed Fabs. These Fab solutions were subsequently combined with biotin-labeled Fab (660 ng/mL) in a 1:1 volume ratio. Fab solution (100 μL) was added into the wells and incubated for 2 h at room temperature. After triple washing, streptavidin-horseradish peroxidase (100 μL, 20 ng/mL in ELISA buffer) was introduced and incubated for 45 min at 37 °C. Post six washes, TMB substrate (100 μL) was added, followed by a

15-min incubation period and the addition of phosphoric acid (100 μL, 1 M). The plate was subsequently analyzed at an absorbance of 450 nm utilizing a SpectraMax® plate reader (Molecular device, USA).

2.4. In vivo studies

All experimental protocols were approved by and performed in accordance with the local animal committee (2021/UCL/MD/030 and 2024/UCL/MD/020) and as specified by the Belgian Law of 29 May 2013 on the protection of laboratory animals.

2.4.1. Foam retention and distribution

Six-week-old male C57BL/6J mice (20–25 g) were purchased from Janvier Laboratories, France. Animals were randomly divided into two groups and housed in a controlled environment (room temperature of 23 ± 2 °C, 12 h daylight cycle) with *ab libitum* food intake and sterile water. To evaluate *in vivo* foam adhesion, C57BL/6 mice were administered with basic pre-foam (40 μL) containing Fab (25 mg/mL) and acidic pre-foam solution (40 μL) rectally. Colonoscopic images were captured at specific time intervals, and the residual foam was examined. Foam adhesion was evaluated using IVIS and fluorescently labeled Fab (described in Supplementary Information). Mice were anesthetized with isoflurane and received acidic pre-foam solution (40 μL) and basic pre-foam solution (40 μL) containing fluorescein-labeled Fab (25 μg/mL) rectally at a dose of 1 mg /25 g mouse. Mice were imaged employing an IVIS Illumina XMRS camera (Perkin-Elmer, USA) after 30 min and 2 h post-administration (4 mice per group).

To determine the Fab concentration in colon, mice were euthanized 30 min after administration of Fab solution, FabF and FabLF (5 mice per group, 1 mg/mouse). Colon was then harvested and dissected into two segments with equal length, labeled as proximal and distal. Lysis buffer was prepared, comprising NaCl (500 mM), EDTA (2 mM), 1% Triton X-100, 0.5% sodium deoxycholic acid, 0.1% SDS, protease inhibitor cocktail, and Tris-HCl (50 mM) in Milli-Q water. The dissected colon was weighed while remaining frozen. Then, 300 mg of tissue per mL of cold lysis buffer was added. Tissues were homogenized with a homogenizer at 4000 *g* for 1 min, with four cycles at 4 °C and then centrifuged at 100,000 *g* for 20 min. Fab concentration in colon was measured *via* a customized ELISA using a MULTI-ARRAY® 96-well plate (MesoScale Discovery, USA). The detailed method is included within the Supplementary Information. The plate was read using a MESO QuickPlex SQ 120 plate reader (MesoScale Discovery, USA). Results were normalized to the overall protein concentration in the buffer using a Pierce™ BCA Protein Assay Kit.

2.4.2. Pharmacokinetics study

Six-week-old male C57BL/6J mice (20–25 g) were purchased from Janvier Laboratories, France. Animals were randomly divided into two groups and housed in a controlled environment (room temperature of 23 ± 2 °C, 12 h daylight cycle) with *ab libitum* food intake and sterile water (5 mice per group). Mice were administered with Fab solution and FabF at a 1 mg/mouse Fab dose. At different time points (0, 0.25, 0.5, 1, 2 and 4 h), blood samples were collected from the tip of the tail vein, which were then centrifuged at 1500 *g* for 10 min, and the Fab plasma concentration was quantified using the ELISA method described in section 2.4.1.

2.4.3. In vivo murine colitis models

Six-week-old male mice were purchased from Janvier Laboratories, France and housed in a controlled environment (room temperature of 23 ± 2 °C, 12 h daylight cycle) with *ab libitum* food intake and sterile water. Chemically-induced murine colitis models were developed following previously reported dosages/regimens (8 mice per group).[15] In the acute dextran sodium sulfate (DSS) model, disparate degrees of colon inflammation were induced by adding distinct concentrations of DSS in drinking water. Mild and severe colitis were induced using 3% and 5% DSS solutions, respectively, in drinking water for 5 days. The DSS solution was replaced every other day, while the healthy control group received only water. Rectal foam administration to the mice was conducted under anesthesia *via* isoflurane, with a 1 mg/mouse dose on days 3 and 6 of the experiment. On day 6, DSS water was replaced with fresh water, and mice were sacrificed on day 8 for further analysis.

In the 2,4,6-Trinitrobenzene sulfonic acid (TNBS) acute model, mice underwent a 12-h fasting period before intrarectal TNBS administration. Mice (10 mice/group) were anesthetized with isoflurane, and TNBS (100 mg/kg, in 0.9% NaCl-ethanol, 50:50, *v*/v) was intrarectally administered to induce colitis. Healthy mice received a solution of 0.9% NaCl-ethanol (50 μL, 50:50, v/v). On the second day post-TNBS injection, foam was rectally administered to mice at a 1 mg/mouse Fab dose. Mice were euthanized on day 4 for subsequent analysis.

In the chronic mice model (8 mice/group), colitis was induced by 3% DSS in drinking water for 7 consecutive days, with the solution replaced every other day. On day 8, DSS water was substituted with fresh water for 2 weeks to facilitate recovery. This process was repeated for two additional DSS cycles. Specifically, at week 4, DSS concentration was re-introduced at 3% for 7 days, followed by a 2-week DSS-free period. DSS was then re-introduced for 7 days during week 7, after which mice were humanely euthanized for further study. Healthy mice had access to water during the entire experiment. This chronic model emulates human inflammatory bowel disease clinical manifestations, providing a more accurate model for evaluating potential treatments. Foam treatment started during week 4 and was rectally administered to mice on days 3 and 6 of the week with a 1 mg/mouse dose.

On the final day, a colonoscopy video was recorded to assess disease severity index, with scoring standards outlined in our previous publication.[16] This process was conducted by a gastroenterologist (T. Moreels) in a single-blinded manner. While anesthesized, blood was collected *via* cardiopuncture, and mice were humanely euthanized. The colon was harvested, rinsed with PBS to remove feces, and the cecum was discarded. The colon length and weight were measured to calculate the colon weight/length ratio. The colon was then sectioned into multiple pieces for further analyses.

2.4.4. In vivo efficacy evaluation

The weight of the mice was measured starting from day 1. The percentage of weight loss was calculated by dividing the current weight by the initial weight on the first day. This percentage was recorded throughout the entire experimental procedure.

Colon was homogenized using the same method as described in section 2.4.1. To assess cytokine concentrations in colon tissue, the concentrations of the series of colonic pro-inflammatory cytokines and chemokines were determined with a V-PLEX Plus Mouse Cytokine 19-Plex ELISA kit (MesoScale Discovery, USA) following the manufacturer's instructions using a MESO QuickPlex SQ 120 plate reader (MesoScale Discovery, USA). Specifically, lysis buffer was prepared as described in section 2.4.1. The dissected colon was weighed while remaining frozen. Then, 150 mg of tissue per mL of cold lysis buffer was added. Tissues were homogenized using the aforementioned method and then centrifuged at 100,000 *g* for 20 min. An aliquot of the supernatant (25 μL) was collected and analyzed to determine cytokine concentration in the tissue. The results were normalized to the protein content, quantified with a Pierce™ BCA Protein Assay Kit.

Histological scoring was performed following a previously described method.[17] Colon segments were initially fixed overnight in 4% buffered formalin, then sequentially washed with 70% ethanol, and embedded in paraffin. These sections underwent hematoxylin-eosin (H&E) staining for histological evaluation, adhering to the histopathologic criteria established by Koelink et al.[18]

2.5. Non-everted gut ex vivo study

The *ex vivo* studies were conducted in adherence to the University

College Dublin (UCD) Animal Research Ethics Committee Protocol #14–28. Colonic segments were extracted from euthanized rats as previously described,[19] and promptly immersed in pre-oxygenated, warm Medium 199. The fecal content was gently expelled from the colon. In line with established methods, sacs in a non-everted configuration were prepared, yielding two to three sacs per colon, each approximately 5.5 cm in length.[19]

Our investigation encompassed various groups, including a mixture of the emulsifier (containing all foam components except those enabling gas generation), two gas solution (a blend of PB and CA, mirroring the compositions of LF and foam respectively), foam and LF variants themselves and C_{10}. One end of each colon sac was sealed with surgical suture. Initially, composition with out fluorescein isothiocyanate (FITC)-dextran (FD) was introduced into the lumen (40 μL). Subsequently, the other end was loosely tied, allowing for needle insertion without tissue penetration. Solutions containing FD were then injected in the same volume as the initial solution. Following rapid needle retraction, the sac was securely sealed. Each sac was individually placed in an organ bath at 37 °C, containing oxygenated Medium 199 (8 mL). The medium was gassed with 95% of O_2 and 5% of CO_2. Sample collection from the bath medium occurred at regular intervals: initially every 1 min for the first 5 min, then every 5 min up to 30 min, and subsequently every 10 min until the 90-min mark. These samples were directly transferred onto a Nunclon® 96-well white Maxisorp plate (Thermo Scientific, USA), and the FITC signal intensity was measured as previously described.[19] Post-experiment, the gut sacs were preserved in 10% formalin and subjected to H&E staining. The stained samples were then examined under a microscope for histological analysis.

2.6. Statistical analysis

The statistical analysis in our study was carried out using GraphPad Prism 9 software (USA). Grubbs test was applied to identify and support the exclusion of any outliers in each group. Depending on the homogeneity of variances, as determined by the Brown-Forsythe test, we utilized either two-way or one-way ANOVA, followed by Tukey's post-hoc test for multiple group comparisons. In cases where significant variance differences were observed between groups, we conducted a nonparametric analysis. For comparing two groups specifically, Student's *t*-test was applied. Results were presented as the mean ± standard error of the mean (SEM). A *p*-value (*p) of <0.05 was set as the threshold for statistical significance.

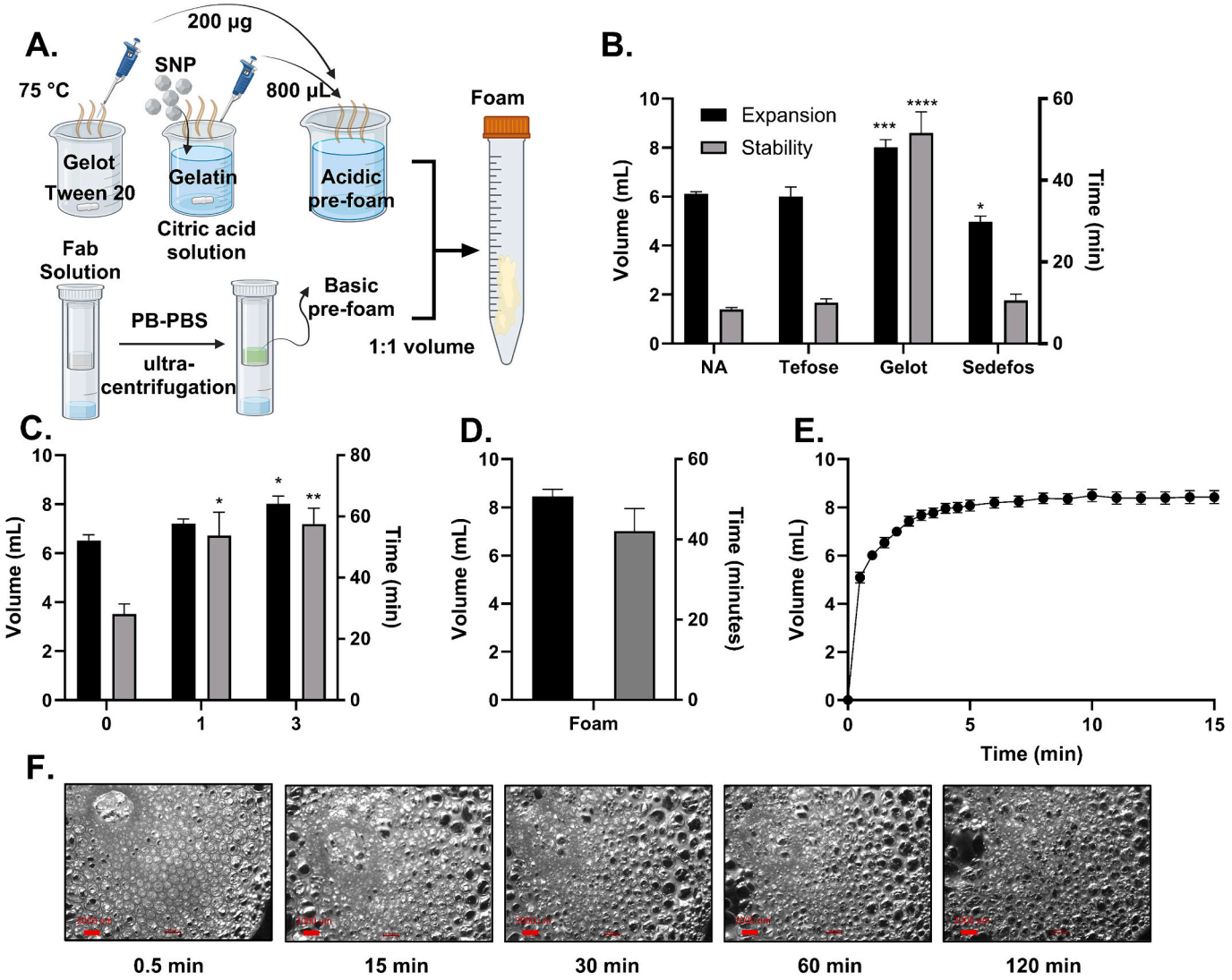

Fig. 1. Physico-chemical characterization of the foam. A) Schematic of the preparation of the foam. B) Effect of foaming emulsifiers on the expansion and stability of the foam ($n = 7$). C) Effect of SNP concentrations on the expansion and the stability of the foam (n = 7). D) The expansion and the stability of the foam ($n = 9$). E) Expansion kinetic of the foam (n = 9). F) Time-coursed microscopic image of the foam. Statistical analysis was conducted *via* a Student's *t*-test. Results were presented as the mean ± standard error of the mean (SEM).

3. Results

The foam was prepared through mixing two pre-foam solutions, a basic and an acidic, consisting of PB and CA, respectively, resulting in a chemical effervescence system. A solution of 3 M PB, a close-saturated PB solution, and a solution of 1.6 M CA were used to maximize gas generation. The fabrication of the foam was demonstrated as Fig. 1A. The foam composition was further optimized. Our primary focus was on foams with the greatest volumetric expansion which exhibited prolonged stability. A series of surfactants and foaming reagents were evaluated for their efficacy at enhancing the foam's expansion and its temporal stability. Among the selected excipients, the non-ionic emulsifier, polysorbate 20 (Tween® 20), promoted the highest degree of foam expansion with stability over 40 min (Supplementary Information, Fig. S1). The oil-in-water emulsifier, Gelot™ 64, was also identified as an additional critical component in the preparation of a stable foam matrix to enhance foam stability (Gelot™ 64 *vs* no Gelot™ 64, $^{****}p < 0.0001$, Fig. 1B.). We incorporated silica nanoparticles (SNP) into our foam formulation, a technique commonly employed in industry to stabilize foams, but not yet to our knowledge applied in pharmaceutical foams.[20] The integration of silica nanoparticles at a concentration of 3 mg/mL amplified foam expansion by 1.3-fold and doubled its stability duration (Fig. 1C). The stability and volumetric expansion of the optimized foam are illustrated in Fig. 1D. The foam expanded up to 8 mL, ~ 20 times the volume of the original pre-foam mixture. The composition enabled the foam to be maintained *in vitro* for ~40 min. Expansion was not immediate; it took 6 min to attain full volume, as shown in its kinetic profile (Fig. 1E). Microscopic examination of foam bubbles on a glass slide, presented in Fig. 1F, revealed that while the overall bubble frame and size were maintained for up to 2 h (Supplementary Information Fig. S2), foam deformation and collapse began at 30-min. Further analysis of the foam's rheological properties indicated that the foam behaved as a viscoelastic solid-like material (Supplementary Information, Fig. S3).

We then loaded an anti-TNF-α Fab into the foam. To ensure the stability of the anti-TNF-α Fab in this solution, we monitored its intrinsic fluorescence and optical density for over two months (Fig. 2). The quaternary structure of the Fab is crucial for its efficacy. The unfolding of the Fab was evaluated by observing the red shift in the intrinsic fluorescence maximum emission wavelength. Guanidine hydrochloride was used to completely unfold the antibody. As demonstrated in Fig. 2A, the Fab in the basic pre-foam formulation showed no change in its maximum emission wavelength, suggesting that the basic pre-foam solution did not affect the quaternary structure of the Fab. The aggregation of the Fab was then tested using UV methods. The optical density of Fab in the basic pre-foam formulation was compared with that of newly thawed Fab, and identical spectra were observed (Fig. 2B). This result was also validated *via* a turbidity test (Fig. 2C). Turbidity was measured by UV absorbance at 340 nm, and there was no increase in Fab in basic pre-foam formulation compared with newly thawed Fab. These results confirmed that Fab remained stable when stored in the basic pre-foam solution. Given that the Fab's therapeutic action in treating colitis requires the neutralization of TNF-α through association, we evaluated whether its binding affinity to TNF-α was preserved post-foaming *via* a competitive binding ELISA. The results, depicted in Fig. 2D, showed that the inhibition curves of the Fab post-foaming aligned with those of the freshly thawed unformulated Fab. Moreover, the IC_{50} values for both the post-foam Fab and the freshly thawed Fab were similar ($p > 0.05$; Fig. 2E), indicating no loss in binding affinity during the foaming process. These results supported our hypothesis that this foam system could be used as a potential delivery vehicle without compromising the therapeutic efficacy of Fab even with the generation of water-gas interface.

We then investigated both local and systemic *in vivo* behavior of the foam formulation. Foam was administered rectally to healthy mice. A colonoscopy set was utilized to examine the Fab-loaded foam (FabF) adhesion to the colon wall over time. As illustrated in Fig. 3A, FabF enabled colon adherence for up to 2 h, with residual foam still visible after 4 h. The foam distributed along the colon lining in a homogeneous pattern. For further visualization of the Fab distribution post-foaming, we labeled the Fab with FITC (FITC-Fab), and used an IVIS® system to

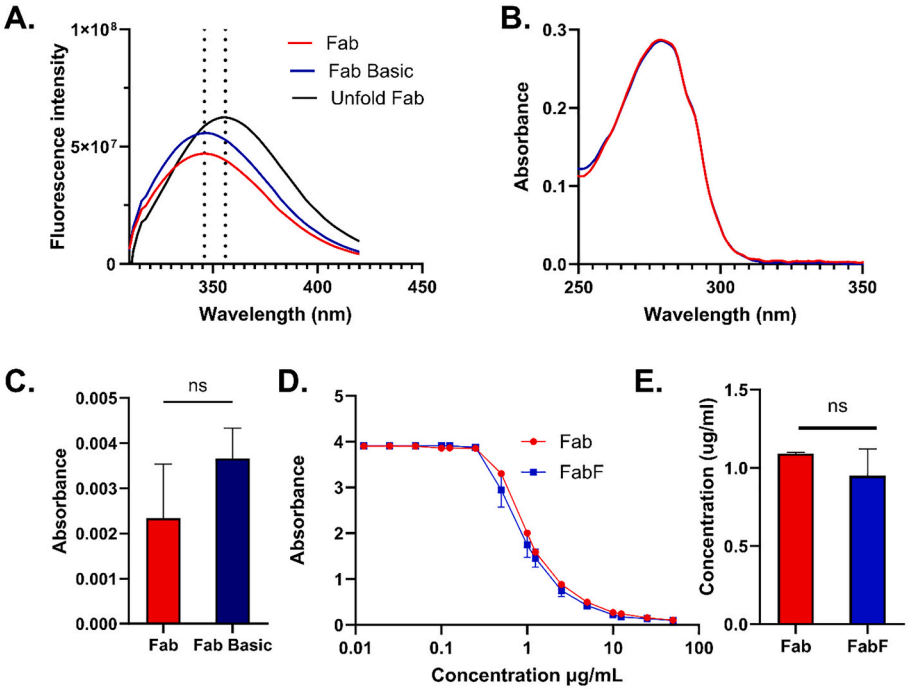

Fig. 2. Stability of Fab in foam A) Intrinsic fluorescence spectrum of Fab and Fab in basic pre-foam formulation (Fab basic) after 2 months at 4 °C. ($n = 3$) B) Optical density of Fab and Fab basic after 2 months at 4 °C. (n = 3) C) Turbidity of Fab basic after 2 months at 4 °C. (n = 3) D) Inhibition curve of the Fab post-foaming process compared with newly thawed Fab (n = 3). E) IC_{50} for binding affinity of Fab post-foaming and newly thawed Fab (n = 3). Statistical analysis was conducted *via* a Student's *t*-test. Results were presented as the mean ± standard error of the mean (SEM).

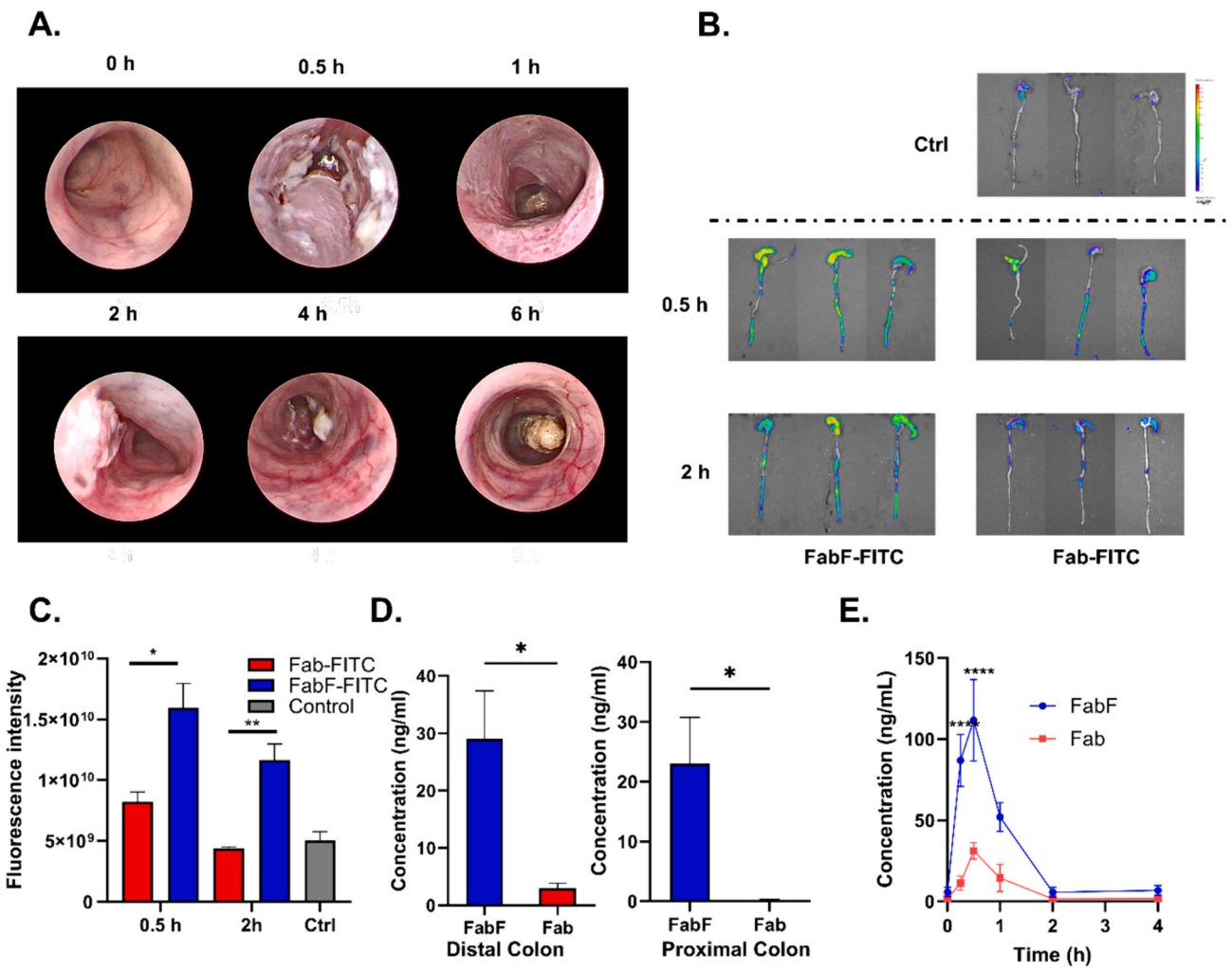

Fig. 3. Local and systemic distribution of Fab in colon facilitated by the foam in mice following rectal administration. A) Time-course image of foam adhesion in colon *via* colonoscopy. White arrow points to foam residue after 4 h. B) Retention of FITC-Fab in colon delivered *via* foam formulation and solution by IVIS®. C) Fluorescence intensity of FITC-Fab in murine colon ($n = 3$–4). D) Distribution of Fab in different colon segments ($n = 4$–5). E) Plasma levels of rectally-administered Fab and FabF (n = 4–5). Statistical analysis was performed using Student's *t*-test (C & D) (*$p < 0.05$; **$p < 0.01$) or two-way ANOVA followed by Šídák's multiple comparison test (E) (****$p < 0.0001$). Data are presented as the mean ± SEM.

capture fluorescence intensity within the colon (Fig. 3B and C). Compared to FITC-Fab in solution, mice treated with FITC-FabF displayed higher fluorescence intensity, 1.65-fold at 30 min post-administration (*$p = 0.0115$). After 2 h, fluorescence in the FITC-Fab solution group returned to baseline, whereas the FITC-FabF group retained ~30% of the initial intensity. In addition, we observed pronounced fluorescence in the proximal colon, indicating broad area coverage by FabF. Quantitative analysis confirmed these visual findings (Fig. 3D). Colons were dissected into distal segments and proximal segments. Thirty min post-administration, dissected colons were homogenized to measure FITC-Fab concentrations. The results revealed a substantial increase in FITC-Fab levels in both sections for the FITC-FabF group, up to 10-fold in the distal colon and over a 100-fold in the proximal colon compared to mice receiving rectal FITC-Fab solution (*$p = 0.03$ and *$p = 0.02$, respectively).

A pharmacokinetic (PK) study was conducted to evaluate the impact of the foam on Fab systemic levels. As demonstrated in Fig. 3E, the administration of the rectal foam to mice significantly elevated plasma concentrations of Fab at 15 and 30 min post-administration (Fab solution *vs* FabF, ****$p < 0.0001$). This amounted to an over 4-fold increase in the area under the curve (AUC) for the foam Fab formulation over solution. These findings indicated that the foam not only augments the local distribution of Fab along the murine colon, but also enhances its systemic absorption in colon compared to the solution of the Fab when administered as a rectal enema.

Subsequently, an established acute chemically-induced murine colitis model was used to assess therapeutic efficacy of the rectal FabF. A solution of 3% dextran sodium sulphate (DSS) was added to drinking water for 5 days to induce mild colitis in mice.[21] Fab solution and FabF were rectally-administered twice, at day 3 and day 6 (Fig. 4A). The progression of colitis was monitored by recording the weight loss percentage, illustrated in Fig. 4B. Although the FabF failed to reverse the weight loss of the colitis mice, it would also not aggravate the process. The colonic weight-to-length ratio, an indicator of colonic inflammation, was significantly reduced in the FabF-treated group compared with the colitis control group (Fab *vs* DSS-treated group; ***$p < 0.001$), indicating alleviated inflammation (Fig. 4C). The Fab solution did not yield a comparable reduction (Fab *vs* DSS group, $p > 0.05$). Disease severity was further evaluated using colonoscopic and histological analysis, as shown in Figs. 4D & E, respectively. The murine endoscopic index of colitis severity (MEICS) results indicated a downward trend in disease severity among the FabF-treated group compared to control and Fab-treated groups, although this did not reach statistical significance ($p > 0.05$) (Fig. 4D). Similarly, histological evaluations revealed that the disease severity in the FabF-treated mice was indistinguishable from that of healthy mice (FabF *vs* healthy group, $p > 0.05$), indicating

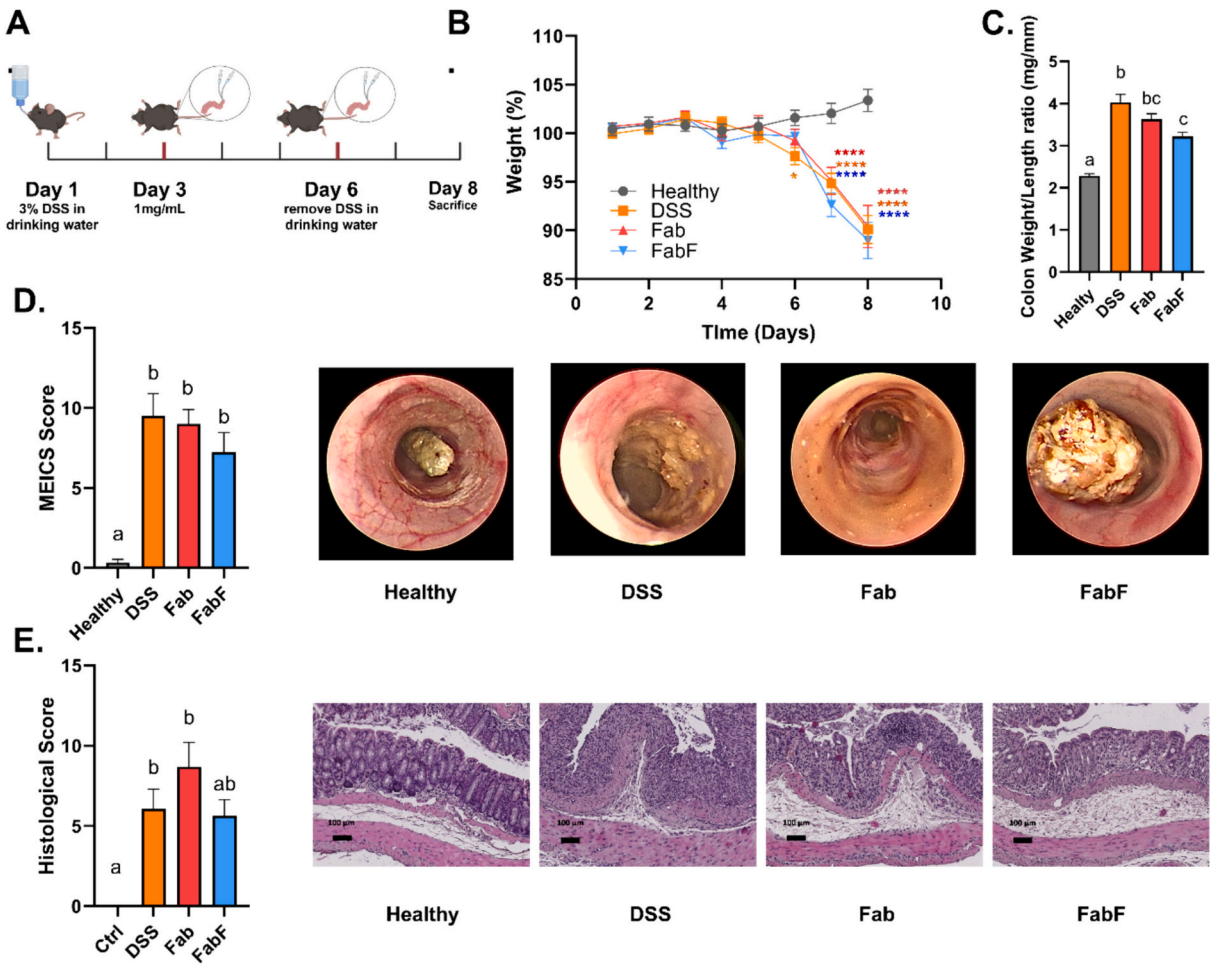

Fig. 4. *In vivo* testing of efficacy of FabF in the DSS murine colitis model. A) Scheme of model construction and dosing for DSS-induced colitis model in which Fab was administered a dose of 1 mg/mouse at day 3 and day 6. B) Weight percentage loss of the mice (n = 6–8). C) Colon weight to length ratio (n = 6–8). D) Murine endoscopic index of colitis severity (MEICS) evaluated by colonoscopy (n = 6–8) and representative colonoscopy images per group. E) Histological analysis (n = 6–8) and representative histological images per group, scale bar = 100 μm. Statistical analysis was performed using a two-way ANOVA followed by Tukey's multiple comparison test (B), one-way ANOVA followed by Tukey's multiple comparison test (C) or Kruskal-Wallis test followed by Dunn's multiple comparison test (D&E). The letters (a, b, ab, *etc.*) represent the results of Tukey's multiple comparison or Dunn's multiple comparsion. They are a shorthand to show which groups' means are significantly different from each other. Data are presented as the mean ± SEM.

efficacy of FabF (Fig. 4E). Conversely, according to histology read-outs, the Fab solution did not demonstrate efficacy.

We extended our investigation of FabF efficacy to two acute severe colitis disease models: one induced by 5% DSS drinking water (Supplementary information, Fig. S8) and another by rectal 2,4,6-Trinitrobenzene sulfonic acid (TNBS) administration (Fig. 5).[21] In the 5% DSS model, the protocol was analogous to the one described above for 3% DSS. For the TNBS model, rectal administration of FabF or Fab was followed by treatment on the second day (1 mg Fab/mouse), with the protocol outlined in Fig. 5A. Mice weight loss percentages were monitored over the treatment period (Supplementary information, Fig. S6). Although the FabF-treated mice did not achieve a positive response in the 5% DSS model (Supplementary information, Fig. S7), in the TNBS model, FabF ameliorated the weight-to-length ratio of the colon compared to the colitis control group ($p = 0.04$), as shown in Fig. 5B. MEICS scores in the TNBS model also indicated a similar disease severity compared with healthy mice (FabF *vs* Healthy, $p > 0.05$; TNBS *vs* Healthy, $^*p < 0.05$) (Fig. 4C). In both of these severe murine colitis models, FabF did not alleviate disease severity using histological analysis (Fig. 5D).

Further therapeutic efficacy assessment was conducted by quantifying pro-inflammatory cytokines (TNF-α, IL1β, IL-6, and KC/GRO) in colon tissues (Fig. 6). The chemically induced murine colitis models produced uneven effects in the colon from the two models, more severe at the distal end and less so at the proximal end.[21] Due to this heterogeneous distribution, colon sections were collected from the proximal and distal ends, respectively. Remarkably, in both the 5% DSS and TNBS models, FabF treatment resulted in reduced cytokine levels in the proximal colon, as illustrated in Fig. 6A. Specifically, in the proximal colon of mice subjected to 5% DSS and treated with FabF, there was a reduction, exceeding 70%, in the levels of all four measured cytokines. The decrease in TNF-α surpassed 75% compared to the colitis control, albeit without statistical significance. Most notably, IL-1β concentrations were significantly lowered by >90% with FabF treatment compared to the DSS group ($p = 0.0294$). Levels of IL-6 and KC/GRO were comparable to those in healthy mice. A similar pattern was observed in the TNBS model, where FabF treatment led to a reduction in pro-inflammatory cytokines by >25% in the proximal colon. Specifically, TNF-α and IL-6 levels in the proximal colon were decreased to a similar level in healthy mice ($P > 0.05$, FabF *vs* Healthy). FabF treatment did not reduce pro-inflammatory cytokine levels in the distal colon (Fig. 6B). However, TNF-α levels in the distal colon showed a decreasing trend in both the DSS and TNBS models, comparable to those in healthy mice (P > 0.05, FabF *vs* Healthy). Furthermore, MPO levels were assessed in both the distal and proximal colon. In both models, no significant differences were observed between groups in the proximal

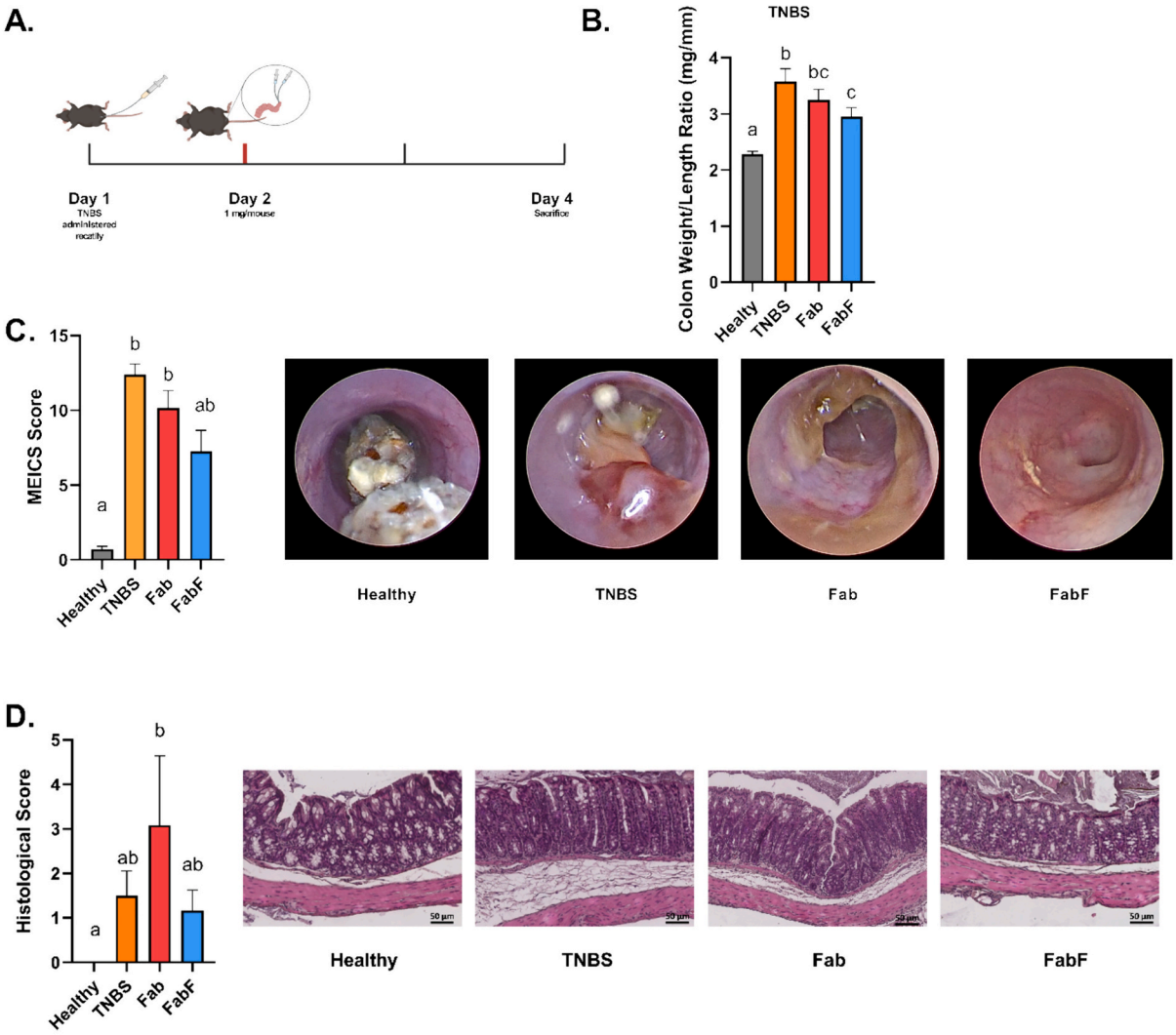

Fig. 5. *In vivo* efficacy testing of FabF in severe acute colitis model induced by TNBS. A) Scheme of the TNBS-induced colitis model and dosing in which Fab was administered at a dose of 1 mg/mouse once at day 2. B) Colon length-to weight ratio (n = 6–10). C) MEICS scores (n = 6–10) and representative images per group. D) Histologic analyis (n = 5–10) and representative images per group, scale bar represented 100 µm. Statistical analysis was performed using a one-way ANOVA followed by Tukey's multiple comparison test (B) or Kruskal-Wallis test (C&D) followed by Dunn's multiple comparison test. The letters (a, b, ab, *etc.*) represent the results of Tukey's multiple comparison or Dunn's multiple comparsion. They are a shorthand to show which groups' means are significantly different from each other. Data are presented as the mean ± SEM.

colon. In contrast, neither Fab nor FabF treatments effectively reduced MPO levels in the distal colon (Supplementary Information, Fig. S8).

To better emulate the clinical scenario of IBD, we tested our foam formulation in a chronic colitis mouse model. As our prototype foam formulation reached maximal expansion capacity due to the saturation of PB, we introduced a variation that produced less CO_2, designated as low foam (LF). The properties of this LF foam are described in Suplemmentary information Fig. S4 and Fig. S5. The chronic colitis model was induced using 3% DSS in the drinking water, with a longer experimental timeline and dosing regimen depicted in Fig. S10A. FabF and Fab-loaded LF (FabLF) were rectally administered to groups of mice alongside with unloaded original foam and unloaded LF as controls. As for our previous acute mouse colitis studies, a Fab solution control was also administered rectally. Weight loss was monitored throughout, and towards the last DSS cycle, a diminishing trend in weight loss was noted for groups treated with FabF, FabLF, and the Fab solution, although no significant differences were observed between the groups (Fig. S6). No changes were observed in the colon weight-to-length ratios (Fig. S10B). Mice receiving FabF and FabLF demonstrated improved endoscopic MEICS scores (*t*-test; FabLF *vs* DSS, $p = 0.02$; FabF *vs* DSS, $p = 0.032$) (Fig. S10C&E). Similar data was observed in the histological score for FabLF-treated mice, where improved inflammation condition was noted (*t*-test; FabLF *vs* DSS, $p = 0.023$) (Fig. S10D&F). However, statistical significances in both analyses were lost using Kruskal-Wallis test ($p > 0.05$) followed by Dunn's *post hoc* test. No differences were observed with the rest of the treated groups. These results demonstrated that, based on macroscopic standards, both FabF and FabLF failed to ameliorate chronic inflammation in the colon. However, a trend of decreased MEICS and improved histological images demonstrated the potential of FabLF in treating chronic colitis. It is also noteworthy that rectal Fab solution showed even no trend of therapeutic effect towards colitis mice.

In this study evaluating the efficacy of our foam in chronic colitis, both FabF and FabLF yielded significant reductions in inflammatory markers compared to colitis mice within the distal colon, demonstrating their therapeutic potential (Fig. 7A). In detail, both the FabF and FabLF formulations substantially decreased TNF-α levels >60% compared to the DSS group ($p = 0.036$ for FabF and $p = 0.022$ for FabLF). Additionally, the FabLF formulation also achieved a 90% reduction in IL-6 levels compared to untreated colitis mice ($p = 0.0499$), and similarly,

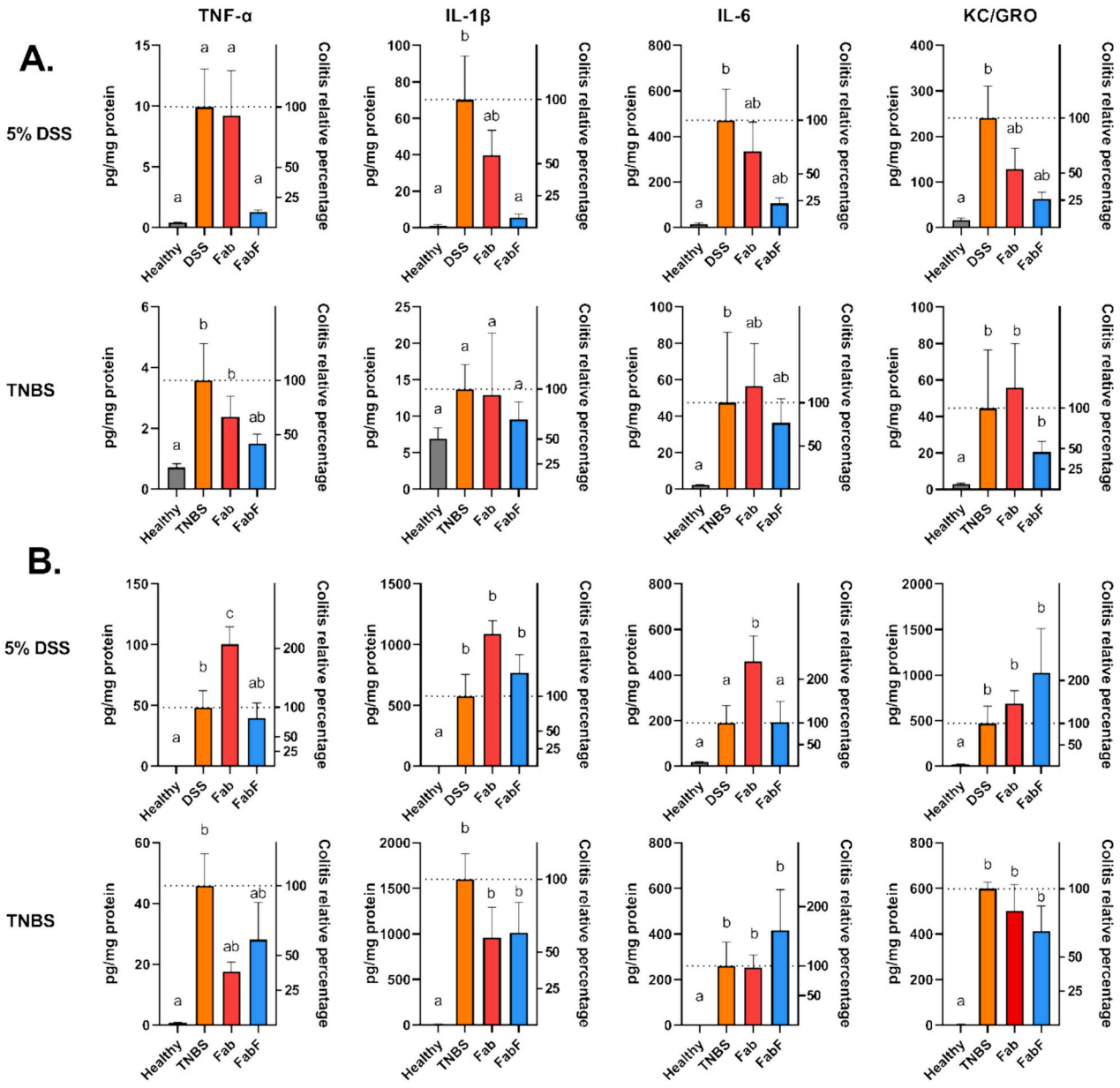

Fig. 6. Pro-inflammatory cytokine TNF-α, IL-1β, IL-6, and KC/GRO in the colon in acute murine colitis models, 5% DSS and TNBS. Colitis relative percentage referred to pro-inflammatory cytokine concentration in colitis group as 100%. A) Pro-inflammatory cytokine levels in proximal colon (n = 5–10). B) Pro-inflammatory cytokine levels in distal colon (n = 5–10). Statistical analysis was conducted *via* one-way ANOVA followed by Tukey's multiple comparison test or Kruskal-Wallis test followed by Dunn's multiple comparison test. The letters (a, b, ab, *etc.*) represent the results of Tukey's multiple comparison or Dunn's multiple comparsion. They are a shorthand to show which groups' means are significantly different from each other. Data are presented as mean ± SEM.

we observed a 70% reduction in KC/GRO cytokine levels in mice treated with FabLF when compared to colitis mice (t-test, $p = 0.038$), although the significant difference was lost when analyzed with Kruskal-Wallis test followed by Dunn's multiple comparison. In contrast, cytokine levels in the proximal colon did not exhibit differences, with even the colitis control group exhibiting low levels comparable to healthy mice. We also extended our analysis to include other chemokines such as MIP-1α. Here, only the FabLF group showed a significant reduction when compared with the colitis control ($p = 0.042$, Fig. 7B). Collectively, these reductions in inflammatory markers in the colon provide evidence of the therapeutic benefits offered by both FabF and FabLF in a chronic colitis model. Despite the difference in the CO_2 composition in FabF and FabLF, their therapeutic effects seemed comparable. We have observed that both FabF and FabLF could adhere to colon in the DSS model over 2 h (Supplementary information, Fig. S11), suggesting the difference of CO_2 production had no effect on the main characteristic of the formulation. Regarding MPO levels, all seven tested groups showed similar levels in the proximal colon. However, in the distal colon, mice treated with only DSS demonstrated significantly higher MPO levels compared to all other groups (Supplementary Information, Fig. S8). In summary, FabLF demonstrated the most potent therapeutic effect in the chronic colitis model. Although FabF also showed some therapeutic effect, it was less pronounced. The Fab solution exhibited only minor therapeutic effects. These results validate that the foam formulation can significantly enhance the therapeutic effect of rectally- administered Fab.

We subsequently explored which specific composition of the foam led to the enhanced plasma concentration of Fab. We ascribed to Tween® 20, which has been used as a permeation enhancer in previous studies.[22] To validate this hypothesis, and to elucidate the contribution of each excipient to this effect, we conducted *ex vivo* studies in isolated

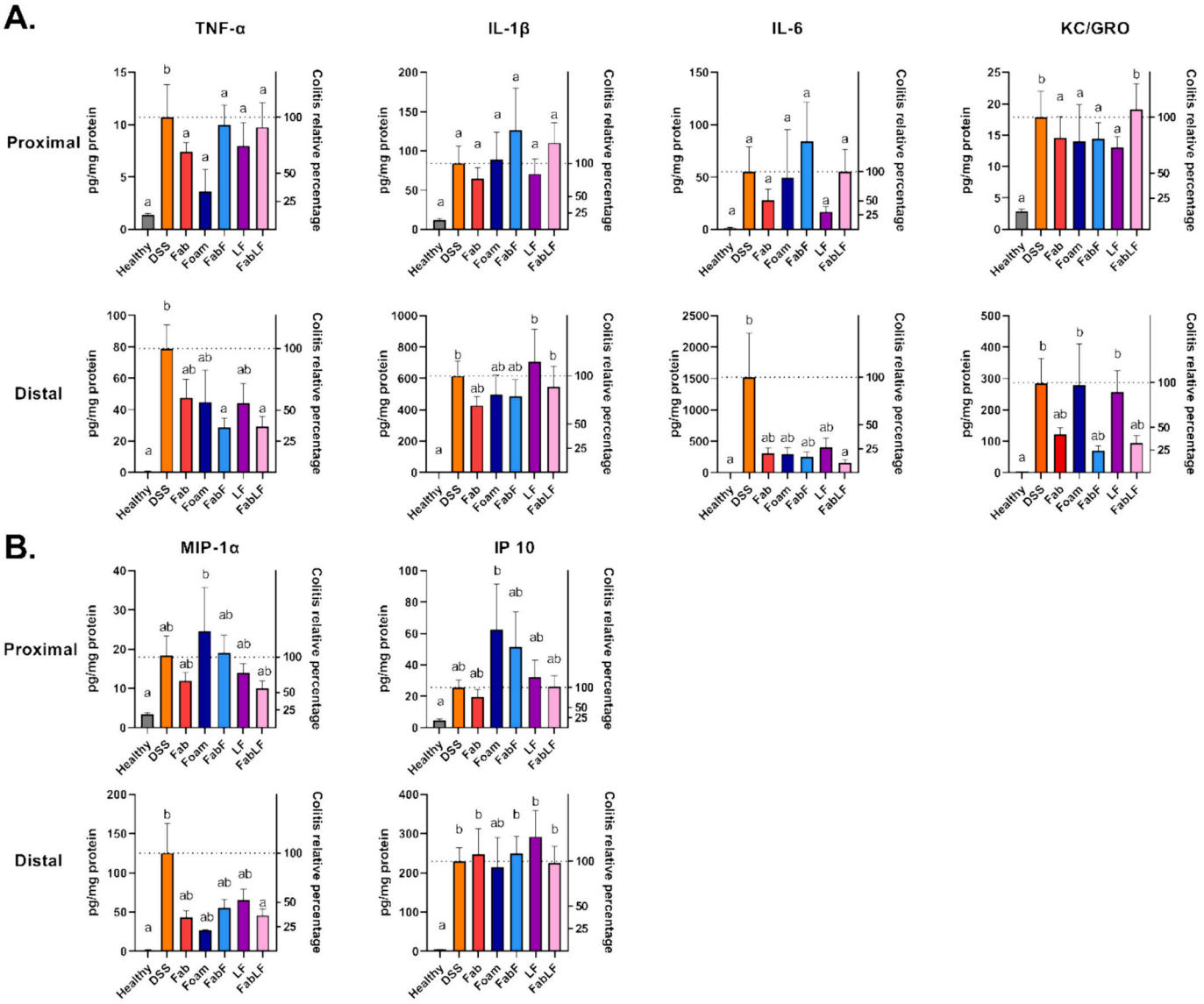

Fig. 7. Pro-inflammatory cytokines TNF-α, IL-1β, IL-6, and KC/GRO and chemokines MIP-1α, IP-10, MCP-1α in the proximal and distal colon following chronic treatment in the DSS-induced colitis model. A) Pro-inflammatory cytokine concentrations in proximal and distal colon ($n = 4–7$). B) Chemokine concentrations in proximal and distal colon (n = 4–7). Statistical analysis was conducted *via* one way ANOVA followed by Tukey's *post-hoc* test or Kruskal-Wallis test followed by Dunn's multiple comparison test. The letters (a, b, ab, *etc.*) represent the results of Tukey's multiple comparison or Dunn's multiple comparsion. They are a shorthand to show which groups' means are significantly different from each other. Data are presented as mean ± SEM.

rat colon tissue. An Ussing chamber assay was employed to ascertain the potential of foam excipients to enhance the transport of macromolecules across colonic mucosa. The permeability of fluorescently-labeled dextran molecules of 40 kDa (FD40K) and 4 kDa (FD4K) was assessed. FD40K represents comparable size to Fab. Among the foam excipients, Tween® 20 at a concentration of 83 mg/mL (corresponding to the Tween® 20 concentration in the foam) was identified as the sole agent in the foam capable of facilitating the transmucosal passage of FD4K. However, contrary to our preliminary hypothesis, Tween® 20 failed to enhance the transepithelial flux of FD40K (Supplementary information, Fig. S12).

To further study the capacity of the foam to enhance permeability, a non-everted rat gut sac model was used to further evaluate the effects of foam on macromolecule transport (Scheme shown in Supplementary Information, Fig. S13).[23] Foam excipients without CA and PB (referred to as 'emulsifier'), gas volumes equivalent to those found in the original foam and LF formulations, foam and LF, were tested. C_{10}, a recognized permeation enhancer, served as a positive control at a concentration of 10 mM.[24] Fig. 8A indicated a direct relationship between CO_2 content in foam and FD4K transport across colonic sacs. High gas (HG), characterized by a higher CO_2 concentration induced with the same CA and PB as in the foam formulation used in mice studies, significantly enhanced the flux of FD4K from the inside to the outside of the sacs, displaying a more pronounced effect than low gas (LG). This relationship highlights the critical role of CO_2 content in facilitating FD transport. Even though the theoretical gas volume was consistent across foam and HG, and LF and LG, the addition of a foaming reagent appeared to hinder the permeation capacity of FD4K. Despite this, both foam and LF were still effective at enhancing FD4K transport. When analyzing the area under the curve (AUC) at 30 min (Table 1), it was evident that HG boosted the AUC of FD4K, increasing it by approximately 47 fold in comparison to the control group (Ctrl *vs* HG $p < 0.0001$). Foam and LF also demonstrated a substantial increase in the AUC for FD4K, enhancing it by 19 and 13 fold (Ctrl *vs* Foam, $p < 0.0001$; Ctrl *vs* LF, $p = 0.0047$, respectively). This trend was sustained over 90 min. Upon further evaluation at 90 min, a similar correlation between gas content

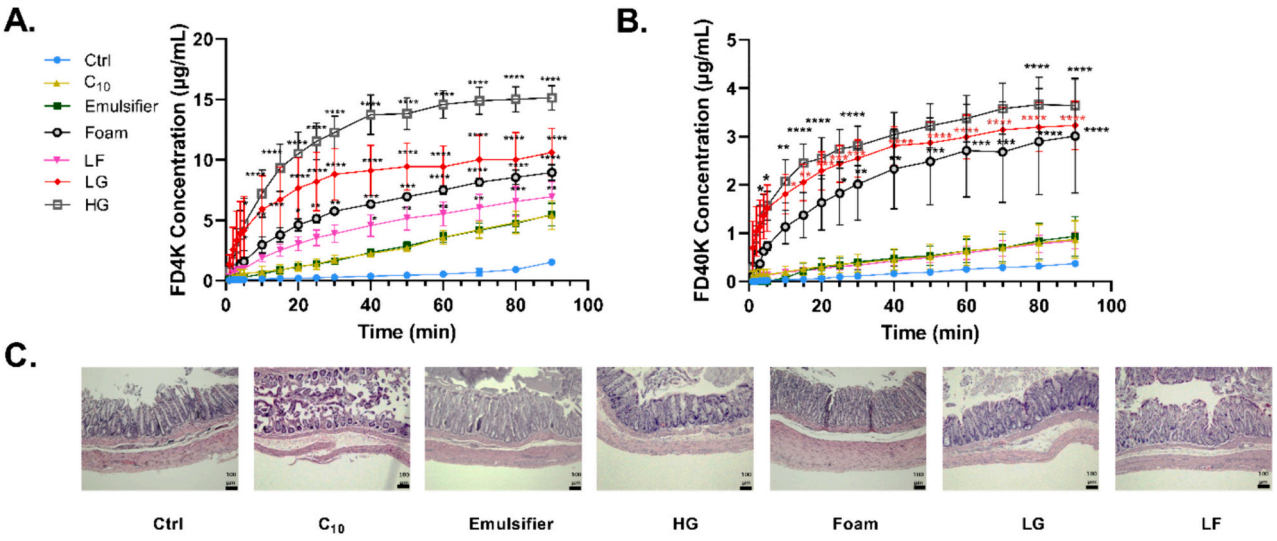

Fig. 8. Evaluation of foam impact on macromolecule transportation across colon in an *ex vivo* non-everted rat gut sac model. A) Effect of foam on transepithelial transport of FD4K from the sac lumen ($n = 3$–4). B) Effect of foam on transport of FD40K from the sac lumen (n = 3–4). C) Representative histology images of colon gut sacs after treatments ($n = 6$–8), scale bar =100 μm. Statistical analysis was conducted *via* two-way ANOVA followed by Tukey's *post hoc* test. Asterisks demonstrated the level of significant difference of Tukey's *post hoc* test compared with Ctrl group. (*, $p < 0.05$; **, $p < 0.01$, ***$p < 0.001$, ****p < 0.0001) Data are presented as the mean ± SEM.

Table 1
AUC of FD4K and FD40K transport across colon in non-everted rat gut sacs.

	Ctrl	C_{10}	Emulsifier	LF	Foam	LG	HG
FD4K 30 min AUC (μg/mL*min)	5.268	28.65	25.64	70.78	104.2	187.5	246.1
FD4K 90 min AUC (μg/mL*min)	44.34	240.8	238.5	458.3	553.2	765.0	1104
FD40K 30 min AUC (μg/mL*min)	1.480	7.488	5.700	6.449	38.27	57.75	64.62
FD40K 30 min AUC (μg/mL*min)	17.51	44.89	44.39	42.21	194.5	236.7	265.6

and AUC was observed, where a greater amount of gas was associated with a larger AUC. All gas-related formulations consistently amplified the AUC by >10 times. In contrast, formulations with only emulsifier or C_{10} led to comparatively lower increases, approximately 5 times larger AUC than the control.

Figure 8B illustrates the transport of FD40K across the gut sac. It was observed that HG, LG, and foam were still effective in altering FD40K permeation. However, LF showed a diminished capacity to sustain this trend when dealing with increased molecular weights. Within the first 30 min, HG significantly enhanced the AUC, achieving a 47-fold increase ($p < 0.0001$), while foam exhibited a 25-fold increase in AUC ($p = 0.021$). This trend remained consistent throughout the duration of the experiment, up to 90 min. Interestingly, as shown in Fig. 8C, compared to gut sacs treated with C_{10}, which resulted in substantial epithelial damage, the gas-containing formulations demonstrated negligible epithelial damage even though they improved permeation of large molecules.

4. Discussion

Rectal foam formulations, until now, have predominantly been used for the administration of small molecule glucocorticoids in the treatment of ulcerative colitis, with a primary focus on maximizing their local therapeutic effects in the sigmoid and transverse colon.[25–27] The potential wider benefits of these types of formulations have been underexplored. We report here the development of a rectal foam to accommodate macromolecular biologics. This innovative approach has successfully demonstrated not only an improved local distribution and retention of a biologic in the colon, but also a significant enhancement in systemic absorption empowered by CO_2 compared to solutions of the biologic.

The gas-water interfaces during the foaming process presented a concern due to their propensity to induce aggregation.[13] Additionally, the use of propellants and pump devices to generate foam has made it challenging to successfully incorporate biologics into foams. Contrary to these concerns, our research has shown that the foaming process of our *in situ* foam could avoid the loss of Fab bioactivity. This could be attributed to two main factors: (1) the design of our foam, which obviates the need for external devices, hence facilitating the loading of biologics, and (2) the inclusion of a non-ionic surfactant, Tween® 20, which acts to stabilize proteins against agitation and minimizes their contact with the interface, thus reducing protein aggregation.[28,29]

The localized administration of therapeutics to the colon is challenged by two significant barriers. Conventional rectally administered therapies to patients with colitis are often quickly expelled due to colon movement and the presence of liquified feces, diminishing local concentration of the treatment.[30] Moreover, the anatomy of the colon can impede the delivery of treatment to its proximal parts. Our foam formulation addresses these issues. The integration of gelatin improved the foam's adhesiveness, ensuring prolonged drug retention within the colon even in non-fasted mice, negating the influence of the feces.

Furthermore, the colon has traditionally been considered a suboptimal site for absorption in the gastrointestinal tract. Its high transepithelial electrical resistance (TEER) and low basal permeability to hydrophilic substances pose a challenge for the permeation of macromolecules, thus limiting its potential as a target for delivery.[24] We have

demonstrated that the foam formulation could significantly enhance the absorption of large molecules *in vivo* such as Fab, prompting a reassessment of the colon as a delivery target where absorption can be promoted.

No single animal model can recapitulate all of the pathogenic and clinical features of human ulcerative colitis.[17] To obtain a deeper comprehension on the therapeutic efficacy of the foam formulation, we applied foams in different murine models based on disease severity and acute/chronic duration. DSS and TNBS models induce colitis-like features *via* distinct mechanisms, with DSS representing innate immune responses in inflammation induction and TNBS illustrating adaptive immune responses in inflammation induction.[21] Additionally, since IBD follows a chronic disease course, acute models do not replicate the pathophysiological situation. Thus, we performed a further investigation using a chronic IBD model, which more closely emulates clinical scenarios. In the severe acute models, the foam formulation displayed reduction of colonic inflammatory cytokines in the less damaged proximal colon (Fig. 6), demonstrating the foam was efficient at reaching and treating this area. In contrast, the chronic model revealed that foam formulation of the Fab displayed increased efficacy in the more severely impacted distal colon. Cytokine concentrations in the proximal colon indicated no differences between healthy and colitis mice (Fig. 7) in chronic model. Remarkably, both FabF and FabLF administrations in the chronic model facilitated a significant diminution of cytokines in the more severely affected distal colon mucosae (Fig. 7). This discrepancy could result from three major factors. (1) Different concentrations of DSS were utilized to induce acute and chronic colitis: 5% DSS for acute colitis and 3% for chronic colitis. This variation likely influenced disease severity and the therapeutic response. (2) In the chronic colitis model, mice received more doses of FabF (eight in total), potentially enhancing its therapeutic effect. (3) FabF was administered during the remission phase in the chronic model, which may have improved its efficacy. This approach aligns with our earlier chronic study, where the previous administration scheme did not involve FabF administration during the washout period and failed to demonstrate amelioration in distal cytokines.

Our research has also deepened understanding of how this foam formulation potentially augments systemic absorption of macromolecules. Effervescent formulations were previously reported to increase the plasma concentration of small molecule drugs.[31,32] However, it was interpreted that this effect comes from the adjustment of pH by the bicarbonate, leading to a higher fraction of the non-ionized form of the drug.[32,33] Eichman et al. reported in 1998 that CO_2 could enhance drug permeation across intestinal mucosae mounted in Ussing chambers.[34] Although CO_2 has been used to improve the transepithelial flux of insulin, this effect was not regarded as a practical or efficacious type of permeation enhancement.[35] This process, requiring continuous CO_2 input towards intestine membrane, resulted in only threefold increase in insulin transport.[35] On the contrary, earlier studies indicated that CO_2 was ineffective in enhancing the permeation of larger biologic molecules, such as Fab, even in the small intestine, a region regarded as being favorable for achieving macromolecule transport.[33] Contrasting with previous studies, our research demonstrates that a single dose of CO_2 significantly enhances FD40K transport across murine colon *ex vivo*, achieving a remarkable 43-fold increase compared to the control group. Additionally, we demonstrated that this permeation enhancement occurred in a rapid manner, showing substantial improvement within 3 min post-administration, kinetics not previously reported (Fig. 8). This implied that the use of CO_2 as a permeation enhancer had the potential to decrease the necessary interaction time with the colon, in contrast to traditional permeation enhancers which typically required a retention time of 2 h in the colon.[24] This enhancement effect correlated directly with the volume of gas and its expansion speed. Increased foam excipient such as Tween 20 and Gelot 64 ratio can prolong the time required to reach maximum expansion of the foam (Supplementary information, Fig. S14). A higher volume of gas and a faster expansion rate resulted in a more pronounced effect. These two factors could contribute to the shear stress, which earlier *in vitro* studies have reported can regulate the openining of tight junctions.[36,37] How to exploit shear stress for enhanced permeation requires further exploration. Intriguingly, our foam formulation avoided the epithelial disruption in the sac model commonly associated with traditional permeation enhancers like C_{10}.[19] This implied that our foam could offer a solution to the long-standing challenge of enhancing permeation without compromising intestinal integrity, although the effects in the long-term upon chronic administration should be further confirmed.

The results of *ex vivo* studies also indicated that the local effect of our formulation plays a dominant role in therapeutic outcomes. This could be explained by two results. First, FabLF demonstrated a reduced capacity to facilitate drug penetration across the colon *ex vivo*, while maintaining therapeutic effects in the chronic colitis model, suggesting that local distribution underpins efficacy. This argument is supported by the improved retention and distribution of the FabLF in colons *in vivo* following rectal administration (Supplementary information, Fig. S4 and S11). Second, although FabF substantially enhanced the murine plasma levels of Fab compared to the Fab in solution, FabF failed to significantly lower pro-inflammatory cytokines in plasma (Supplementary information, Fig. S9). This paradox could be attributed to the short half-life of Fab in plasma.[38] Anti-TNF-α Fab has been applied clinically for IBD treatment in a long acting PEGylated version (Certolizumab pegol) and the Fab required PEGylation to prolong its half-life.[39] While systemic absorption of Fab was improved, overall the therapeutic benefits in the mouse models are primarily due to effects of the formulation in colonic mucosae. In the future studies, biologics with longer half-life should be considered to improve the therapeutical efficacy of foam formulation.

5. Conclusion

In the scope of our research, we have developed an *in situ* foam that incorporates an anti-TNF-α Fab without compromising its biological activity. A rectally-administered formulation markedly enhanced the local distribution and retention of Fab in the murine colon, while also increasing systemic absorption of the Fab. The therapeutic efficacy of the FabF was evaluated across different murine colitis models, ranging from acute to chronic, and from mild to severe. The rectal foam formulation consistently exerted a measurable therapeutic effect in all tested models. The mechanism of action of the foam was elucidated through *ex vivo* rat colonic mucosae studies, which revealed the importance of both the Tween® 20 excipient and CO_2 gas to enhance epithelial permeation, with the gas proving more important in the sac model. Hence, we have devised a novel platform that shows significant promise as a non-injected delivery system to the large intestine for macromolecules in the treatment of IBD.

CRediT authorship contribution statement

Wunan Zhang: Writing – review & editing, Writing – original draft, Methodology, Investigation, Formal analysis, Conceptualization. **Fiona McCartney:** Writing – review & editing, Methodology, Investigation, Conceptualization. **Yining Xu:** Writing – review & editing, Investigation, Conceptualization. **Cécilia Bohns Michalowski:** Investigation. **Inês Domingues:** Investigation. **Espoir K. Kambale:** Investigation. **Tom G. Moreels:** Writing – review & editing, Methodology, Investigation. **Léo Guilbaud:** Investigation. **Cheng Chen:** Investigation. **Valentina Marotti:** Investigation. **David J. Brayden:** Writing – review & editing, Conceptualization. **Ana Beloqui:** Writing – review & editing, Writing – original draft, Visualization, Supervision, Project administration, Methodology, Investigation, Funding acquisition, Formal analysis, Conceptualization.

Declaration of competing interest

There is no conflict of interests.

Data availability

All data relevant to the study are included in the article or uploaded as supplementary information. Complementary data that support the findings of this study are available from the corresponding author, A.B., upon reasonable request.

Acknowledgements

Wunan Zhang is a research fellow from the F.R.S.-FNRS (Fonds de la recherche scientifique, FRIA). Ana Beloqui is research associate from the Belgian FRS-FNRS (Fonds de la Recherche Scientifique) and a WELBIO investigator. Fiona McCartney was a post-doc hired by Gatefossé. This work was supported by the FRS-FNRS (convention J.0010.20), FRFS-WELBIO, with the support of the Wallon region (under grant agreement WELBIO-CR-2022 S–01) and also by CÚRAM, the Science Foundation Ireland Research Centre for Medical Devices, (Grant Number 13/RC/2073_P2), which is co-funded by the European Regional Development Fund. We appreciated the technical support from Estella Isabel Bini and Rose-Marie Goebbels for assistance with histology staining.

Appendix A. Supplementary data

Supplementary data to this article can be found online at https://doi.org/10.1016/j.jconrel.2024.08.023.

References

[1] R. D'Incà, R. Caccaro, Measuring disease activity in Crohn's disease: what is currently available to the clinician, Clin. Exp. Gastroenterol. 7 (2014) 151–161.
[2] D.J. Mulder, et al., A tale of two diseases: the history of inflammatory bowel disease, J. Crohn's Colitis 8 (5) (2014) 341–348.
[3] S. Ghione, et al., Dramatic increase in incidence of ulcerative colitis and Crohn's disease (1988–2011): a population-based study of French adolescents, Off. J. Am. College Gastroenterol.|ACG 113 (2) (2018) 265–272.
[4] T.J. Pasvol, et al., Incidence and prevalence of inflammatory bowel disease in UK primary care: a population-based cohort study, BMJ Open 10 (7) (2020) e036584.
[5] J. Park, J.H. Cheon, Incidence and prevalence of inflammatory bowel disease across Asia, Yonsei Med. J. 62 (2) (2021) 99.
[6] D.C. Baumgart, C. Le Berre, Newer biologic and small-molecule therapies for inflammatory bowel disease, N. Engl. J. Med. 385 (14) (2021) 1302–1315.
[7] J.P. Terdiman, et al., American Gastroenterological Association institute guideline on the use of thiopurines, methotrexate, and anti–TNF-α biologic drugs for the induction and maintenance of remission in inflammatory Crohn's disease, Gastroenterology 145 (6) (2013) 1459–1463.
[8] U.N. Shivaji, et al., Review article: managing the adverse events caused by anti-TNF therapy in inflammatory bowel disease, Aliment. Pharmacol. Ther. 49 (6) (2019) 664–680.
[9] B. Ungar, et al., Optimizing anti-TNF-α therapy: serum levels of infliximab and adalimumab are associated with mucosal healing in patients with inflammatory bowel diseases, Clin. Gastroenterol. Hepatol. 14 (4) (2016) 550–557.e2.
[10] N. Van den Berghe, A. Gils, D. Thomas, Achieving mucosal healing in inflammatory bowel diseases: which drug concentrations need to be targeted? Clin. Pharmacol. Ther. (St. Louis, MO, U. S.) 106 (5) (2019) 945–954.
[11] A. Cortot, et al., Mesalamine Foam Enema Versus Mesalamine Liquid Enema in Active Left-Sided Ulcerative Colitis, Off. J. Am. College Gastroenterol.|ACG 103 (12) (2008).
[12] M. Brunner, et al., Colonic spread and serum pharmacokinetics of budesonide foam in patients with mildly to moderately active ulcerative colitis, Aliment. Pharmacol. Ther. 22 (5) (2005) 463–470.
[13] Y. Xiao, L. Konermann, Protein structural dynamics at the gas/water interface examined by hydrogen exchange mass spectrometry, Protein Sci. 24 (8) (2015) 1247–1256.
[14] S. Mahri, et al., Nebulization of PEGylated recombinant human deoxyribonuclease I using vibrating membrane nebulizers: a technical feasibility study, Eur. J. Pharm. Sci. 189 (2023) 106522.
[15] S. Wirtz, et al., Chemically induced mouse models of acute and chronic intestinal inflammation, Nat. Protoc. 12 (7) (2017) 1295–1309.
[16] C. Becker, M. Fantini, M. Neurath, High resolution colonoscopy in live mice, Nat. Protoc. 1 (6) (2006) 2900–2904.
[17] V. Marotti, et al., A nanoparticle platform for combined mucosal healing and immunomodulation in inflammatory bowel disease treatment, Bioact. Mater. 32 (2024) 206–221.
[18] P.J. Koelink, et al., Development of reliable, valid and responsive scoring systems for endoscopy and histology in animal models for inflammatory bowel disease, J. Crohn's Colitis 12 (7) (2018) 794–803.
[19] C. Twarog, et al., Comparison of the effects of the intestinal permeation enhancers, SNAC and sodium caprate (C10): isolated rat intestinal mucosae and sacs, Eur. J. Pharm. Sci. 158 (2021) 105685.
[20] P. Rattanaudom, et al., Effect of pH on silica nanoparticle-stabilized foam for enhanced oil recovery using carboxylate-based extended surfactants, J. Pet. Sci. Eng. 196 (2021) 107729.
[21] P.K. Randhawa, et al., A review on chemical-induced inflammatory bowel disease models in rodents, Korean J. Physiol. Pharmacol.: Off. J. Korean Physiol. Soc. Korean Soc. Pharmacol. 18 (4) (2014) 279.
[22] A. López, et al., Comparative enhancer effects of span® 20 with tween® 20 and Azone® on the in vitro percutaneous penetration of compounds with different lipophilicities, Int. J. Pharm. 202 (1–2) (2000) 133–140.
[23] S. Keely, et al., In vitro and ex vivo intestinal tissue models to measure mucoadhesion of poly (methacrylate) and N-trimethylated chitosan polymers, Pharm. Res. 22 (2005) 38–49.
[24] F. McCartney, et al., Labrasol® is an efficacious intestinal permeation enhancer across rat intestine: ex vivo and in vivo rat studies, J. Control. Release 310 (2019) 115–126.
[25] H. Courthion, et al., Self-assembling polymeric nanocarriers to target inflammatory lesions in ulcerative colitis, J. Control. Release 275 (2018) 32–39.
[26] J.S. Crowe, et al., Preclinical development of a novel, orally-administered anti-tumour necrosis factor domain antibody for the treatment of inflammatory bowel disease, Sci. Rep. 8 (1) (2018) 4941.
[27] S. Hua, Physiological and pharmaceutical considerations for rectal drug formulations, Front. Pharmacol. 10 (2019) 1196.
[28] Z. Zhang, et al., Adsorption of non-ionic surfactant and monoclonal antibody on siliconized surface studied by neutron reflectometry, J. Colloid Interface Sci. 584 (2021) 429–438.
[29] D.K. Chou, et al., Effects of tween 20® and tween 80® on the stability of Albutropin during agitation, J. Pharm. Sci. 94 (6) (2005) 1368–1381.
[30] M. Mackay, J. Phillips, J. Hastewell, Peptide drug delivery: colonic and rectal absorption, Adv. Drug Deliv. Rev. 28 (2) (1997) 253–273.
[31] G.D. Girolamo, et al., Relative bioavailability of new formulation of paracetamol effervescent powder containing sodium bicarbonate versus paracetamol tablets: a comparative pharmacokinetic study in fed subjects, Expert. Opin. Pharmacother. 8 (15) (2007) 2449–2457.
[32] M. Darwish, E. Hamed, J. Messina, Fentanyl buccal tablet for the treatment of breakthrough pain: pharmacokinetics of buccal mucosa delivery and clinical efficacy, Perspect. Med. Chem. 4 (2010) p. PMC. S3928.
[33] Z. Luo, N. Paunović, J.-C. Leroux, Physical methods for enhancing drug absorption from the gastrointestinal tract, Adv. Drug Deliv. Rev. 175 (2021) 113814.
[34] J.D. Eichman, J.R. Robinson, Mechanistic studies on effervescent-induced permeability enhancement, Pharm. Res. 15 (1998) 925–930.
[35] A.M.M. Sadeghi, et al., Development of a gas empowered drug delivery system for peptide delivery in the small intestine, J. Control. Release 134 (1) (2009) 11–17.
[36] B.S. Conklin, et al., Shear stress regulates occludin and VEGF expression in porcine arterial endothelial cells, J. Surg. Res. 102 (1) (2002) 13–21.
[37] O.C. Colgan, et al., Regulation of bovine brain microvascular endothelial tight junction assembly and barrier function by laminar shear stress, Am. J. Phys. Heart Circ. Phys. 292 (6) (2007) H3190–H3197.
[38] S. Trussel, et al., New strategy for the extension of the serum half-life of antibody fragments, Bioconjug. Chem. 20 (12) (2009) 2286–2292.
[39] G.Y. Melmed, et al., Certolizumab pegol, Nat. Rev. Drug Discov. 7 (8) (2008) 641–642.